Asian Journal of Andrology (2022) 24, 643–652
www.asiaandro.com; www.ajandrology.com

Open Access

ORIGINAL ARTICLE

Prostate Cancer

LncRNA GAS5 enhances tumor stem cell-like medicated sensitivity of paclitaxel and inhibits epithelial-to-mesenchymal transition by targeting the miR-18a-5p/STK4 pathway in prostate cancer

Ting-Ting Lu[1,2,*], Xia Tao[3,*], Hua-Lei Li[4], Ling Gai[5], Hua Huang[6], Feng Li[1]

The onset of prostate cancer (PCa) is often hidden, and recurrence and metastasis are more likely to occur due to chemotherapy resistance. Herein, we identified downregulated long noncoding RNA (lncRNA) growth arrest-specific 5 (GAS5) in PCa that was associated with metastasis and paclitaxel resistance. GAS5 acted as a tumor suppressor in suppressing the proliferation and metastasis of paclitaxel-resistant PCa cells. GAS5 overexpression *in vivo* inhibited the tumor growth of xenografts and elevated PCa sensitivity to paclitaxel. Combination of GAS5 and paclitaxel treatment showed great potential in PCa treatment. Moreover, mechanistic analysis revealed a novel regulatory network of GAS5/miR-18a-5p/serine/threonine kinase 4 (STK4) that inhibits epithelial-to-mesenchymal transition (EMT) and enhances tumor stem cell-like-mediated sensitivity to paclitaxel in PCa. These findings provide a novel direction for the development of a potential adjunct to cancer chemotherapy that aims to improve the sensitivity of chemotherapy drugs in PCa.

Asian Journal of Andrology (2022) **24**, 643–652; doi: 10.4103/aja2021117; published online: 15 March 2022

Keywords: epithelial-to-mesenchymal transition; growth arrest-specific 5; long noncoding RNA; paclitaxel; prostate cancer

INTRODUCTION

Prostate cancer (PCa) is a common, noncutaneous malignant tumor in men with increasing incidence year by year.[1,2] Because of the asymptomatic and unknown characteristics of PCa, patients usually have local invasion or distant metastasis once they exhibit clinical symptoms.[3] Treatment for PCa relies on approaches such as surgery, androgen deprivation therapy, castration therapy, radiation therapy, and chemotherapy.[4] Paclitaxel is a routine taxane-type chemotherapy drug for many cancers,[5,6] including PCa.[7] As in many other cancers,[8,9] paclitaxel chemoresistance is a common problem in PCa treatment,[10] which results in the recurrence and metastasis of PCa, leading to poor survival. Increasing evidence shows that chemoresistance to tumors is largely related to the epithelial-to-mesenchymal transition (EMT) and cancer stem cells (CSCs).[11–13] Therefore, it is necessary to clarify the mechanisms of cancer chemoresistance from this perspective and identify new ways to improve the sensitivity of chemotherapy drugs.

Long noncoding RNAs (lncRNAs) are noncoding RNAs (ncRNAs) with transcripts longer than 200 nucleotides.[14,15] Increasing studies show that lncRNAs participate in many biological processes and functions of gene regulation, such as cell proliferation and differentiation, immune response, miRNA function, and transcriptional regulation.[16–18] LncRNA growth arrest-specific 5 (GAS5) is a common ncRNA that is highly expressed in growth-arrested cells.[19] Reports reveal that GAS5 reverses EMT and tumor stem cell-mediated gemcitabine resistance and metastasis in pancreatic cancer.[20] The molecular mechanisms of GAS5 regulation in PCa are still vague, and in this study, we focused on the mechanisms in which GAS5 participates in inhibiting chemoresistance and metastasis of PCa via regulating EMT and CSC properties.

MicroRNAs (miRNAs) are ncRNAs consisting of 18–25 nucleotides that are involved in posttranscriptional gene silencing by complementary binding to the 3' untranslated regions (3'-UTR) of target genes.[21] Previous studies have reported the dysregulated expression of miRNAs in many cancers.[22,23] Several reports also indicated that miRNAs are involved in the regulation of chemoresistance and metastasis of cancer via regulating EMT and CSC properties.[24–26]

In the present study, we demonstrated that GAS5 expression is downregulated in PCa and is associated with metastasis and paclitaxel resistance. It may play the role of a tumor suppressor in suppressing the proliferation and metastasis of paclitaxel-resistant (PR) PCa cells. *In vivo*, GAS5 overexpression inhibits the tumor growth of xenografts

[1]Department of Laboratory Medicine, Affiliated Hospital of Nantong University, Nantong 226001, China; [2]Department of Pathology, Nantong University Medical School, Nantong 226001, China; [3]Department of Pharmacy, Affiliated Hospital of Nantong University, Nantong 226001, China; [4]Department of Urology, Affiliated Hospital of Nantong University, Nantong 226001, China; [5]Department of Chemotherapy, Affiliated Hospital of Nantong University, Nantong 226001, China; [6]Department of Pathology, Affiliated Hospital of Nantong University, Nantong 226001, China.
[*]These authors contributed equally to this work.
Correspondence: Dr. F Li (lifeng@ntu.edu.cn)
GAS5The pre-print of this paper was published in Research Square in 2021 at website: https://doi.org/10.21203/rs.3.rs-218133/v1.
Received: 08 July 2021; Accepted: 12 December 2021

and elevates PCa sensitivity to paclitaxel. Combination of GAS5 and paclitaxel treatment showed great potential in the treatment of PCa. Moreover, mechanistic analysis indicated that GAS5 inhibited EMT and enhanced tumor stem cell-like-mediated sensitivity of paclitaxel by targeting the miR-18a-5p/serine/threonine kinase 4 (STK4) pathway in PCa. Our data provide novel directions for a potential adjunct to cancer chemotherapy that aimed to improve the sensitivity of chemotherapy drugs in PCa.

MATERIALS AND METHODS

Tissue samples

Thirty-six human PCa samples and 20 benign prostatic hyperplasia tissues were obtained from the Urology Department at the Affiliated Hospital of Nantong University (Nantong, China). The samples were snap-frozen in liquid nitrogen and stored at −80°C. This study was conducted in accordance with the International Ethical Guidelines for Biomedical Research Involving Human Subjects. The protocol was approved by the Ethics Committee of the Affiliated Hospital of Nantong University (approval No. 2020-L052). All participants provided informed consent to participate in this study.

Cell culture

Two PCa cell lines (PC3 and DU145) and RWPE-1 normal human prostate epithelial cells were purchased from the National Collection of Authenticated Cell Cultures (Shanghai, China). All cells were cultured in Roswell Park Memorial Institute 1640 (Gibco, Carlsbad, CA, USA) containing 10% fetal bovine serum (Gibco) and maintained in a humidified atmosphere containing 5% CO_2 at 37°C. PR PCa cell lines (PC3-PR and DU145-PR) were established according to a previous report.[27] Then PC3-PR and DU145-PR cells were cultured in normal medium with 10 nmol l^{-1} paclitaxel (Selleck, Houston, TX, USA).

Drug treatments

For *in vitro* drug treatment experiments, the cultured cells were treated with paclitaxel at 50 μmol l^{-1}, 100 μmol l^{-1}, 200 μmol l^{-1}, 500 μmol l^{-1}, and 1000 μmol l^{-1} for 1 day. After the drug treatments, the cells were used in specific experiments.

Quantitative real-time polymerase chain reaction (qRT-PCR)

Total RNA was extracted using Trizol reagent (Invitrogen, Carlsbad, CA, USA) according to the manufacturer's protocol. Then 1 μg total RNA was reverse-transcribed to cDNA using a First Strand cDNA Synthesis Kit (Applied Biosystems, Foster City, CA, USA). Quantitative amplification was performed using a Step OnePlus Real-Time PCR System (Applied Biosystems). Glyceraldehyde-3-phosphate dehydrogenase (*GAPDH*) or U6 small nuclear RNA (*U6*) was used as an endogenous control. Relative quantification was calculated using the $2^{-\Delta\Delta Ct}$ method. The primer sequences used in this study were as follows: GAS5, forward: 5'-CTTGCCTGGACCAGCTTAAT-3', and reverse: 5'-CAAGCCGACTCTCCATACCT-3'; miR-18a-5p, forward: 5'-TAAGGTGCATCTAGTGCA-3', and reverse: 5'-CAGTGCGTGTCGTGGAGT-3'; *GAPDH*, forward: 5'-GGTGGTCTCCTCTGACTTCAA-3', and reverse: 5'-GTTGCTGTAGCCAAATTCGTTGT-3'; and U6, forward: 5'-CGCTTCGGCAGCACATATAC-3', and reverse: 5'-AACGCTTCACGAATTTGCGT-3'.

Construction of recombinant vector and transfection

Cell transfection was performed using Lipofectamine 3000 Transfection Reagent (Invitrogen) according to the manufacturer's instructions. pCDNA3.1-GAS5 and pCDNA3.1-STK4 overexpression plasmids were constructed and synthesized by Genscript Co., Ltd. (Nanjing, China). The hsa-miR-18a-5p mimic and inhibitor were designed and synthesized by RiboBio Co., Ltd. (Guangzhou, China), miR-CON was designed as a negative control. The luciferase reporter vectors were constructed by RiboBio Co., Ltd. In brief, GAS5 cDNA fragment (based on the GAS5 sequence NR_002578.3 in NCBI, 656 base pairs [bp]) and *STK4* 3'-UTR containing putative potential miR-18a-5p binding sites or mutant sites (based on the sequence NM_001352385.2 in NCBI, 485 bp) were amplified by PCR, and then subcloned into pmiR-RB-Report vector at Xhol and Notl sites (Thermo Fisher Scientific, Cleveland, OH, USA). Site-directed mutagenesis of the miR-18a-5p target sites in the GAS5 cDNA (GAS5-MUT) and *STK4* 3'-UTR (STK4-MUT) were performed using the Quick-Change Mutagenesis Kit (Stratagene, Heidelberg, Germany).

Dual luciferase assay

Cells (2.0×10^4 per well) were seeded into 96-well dishes for 12 h to approximately 70% confluency and then co-transfected with either miR-18a-5p or empty vector and pmiR-RB-Report reporter (pMIR) comprising GAS5 fragment or the 3'-UTR of *STK4* (wild type or mutant) using Lipofectamine 3000 (Invitrogen). After 48 h of transfection, the Dual-Luciferase Reporter Detection System (Promega, Madison, WI, USA) was used to measure luciferase activity according to the manufacturer's instructions.

Cell proliferation assay

Cells (5.0×10^3 per well) were seeded into a 96-well plate and incubated for 24 h, 48 h, and 72 h. Cell viability was determined using a cell counting kit-8 (CCK8) kit (Beyotime Biotechnology, Haimen, China). The absorbance was detected at a wavelength of 450 nm by an Elx800 Reader (Bio-Tek Instruments Inc., Winooski, VT, USA).

Colony formation assay

The PR PCa cells (200 per well) were seeded into a 6-well dish and cultured for 14 days. The cells were fixed with methanol and stained with 0.1% crystal violet (Sigma–Aldrich, St. Louis, MI, USA) for 10 min, and then visible colonies were manually counted.

Migration and invasion assays

For migration assays, transwell chambers were used. Cells (5×10^5 per well) were seeded into the upper chamber of transwell plates without Matrigel (BD Biosciences, San Jose, CA, USA). For transwell invasion assays, diluted Matrigel was added to each upper chamber for 1 h at 37°C. Then the treated cells (5×10^5 per well) were added to the upper chamber and cultured in serum-free medium, and the lower chamber was filled with complete medium. After 24-h incubation, cells that had migrated or invaded through the pores were fixed with 4% paraformaldehyde for 30 min, stained with crystal violet solution for 15 min and then counted.

Flow cytometry analysis

Cells (1×10^6 per well) were seeded into a 6-well plate and cultured for 24 h. Then the trypsinized cells were washed with cold PBS and fixed with 70% ethyl alcohol at 4°C overnight followed by incubation with propidium iodide (0.5 mg ml^{-1}; BD Biosciences) for 15 min. DNA content was detected by a flow cytometer (BD Biosciences).

5-ethynyl-2'-deoxyuridine (EdU) assay

Cells (5×10^4 per well) were seeded into 96-well plates for 48 h at 37°C. Then, 100 μl medium containing 50 μmol l^{-1} EdU (RiboBio Co., Ltd.) was added for another 2 h at 37°C and fixed with 4% paraformaldehyde for 30 min. The fixed cells were permeabilized with 0.5% Triton X-100 (Beyotime Biotechnology, Shanghai, China) for 10 min and

then stained with Apollo 567 (RiboBio Co., Ltd.) and Hoechst33342 (RiboBio Co., Ltd.).

RNA-binding protein immunoprecipitation (RIP) assay

RIP assay was performed using a Magna RIP RNA-Binding Protein Immunoprecipitation kit (Millipore, Burlington, MA, USA) according to the manufacturer's instructions. In brief, the cells were treated with RIP lysis buffer. The cell extract was then incubated at 37°C with RIP buffer (EMD Millipore) overnight with magnetic beads that were conjugated with human anti-IgG (Abcam, Cambridge, UK) or anti-argonaute 2 (Ago2; Abcam) antibodies. With the antibodies recovered by protein A/G beads, the relative expression levels of GAS5 and miR-18a-5p were analyzed by qRT-PCR in the precipitates. IgG was used as a negative control to normalize RNA immunoprecipitates.

Western blotting analysis

Total protein was extracted using a protein extraction kit (Beyotime Biotechnology, Haimen) according to the manufacturer's instructions. Protein concentrations were quantified using a bicinchoninic acid (BCA) kit (Sigma–Aldrich). The protein lysates (40 μg per lane) were separated by 10% polyacrylamide gel electrophoresis and then transferred onto polyvinylidene fluoride (PVDF) membranes (Millipore). Membranes were blocked with 5% fat-free milk containing 0.1% Tween-20 for 1 h at room temperature and then incubated with primary antibodies at 4°C overnight. The following day, membranes were rinsed with Tris-buffered saline plus Tween 20 (TBST) and incubated with the corresponding secondary antibody for 1 h at room temperature. The target bands were scanned and visualized using the chemiluminescence method with a Bio-Rad Gel Doc EZ imager (Life Science Research, Hercules, CA, USA). Image J software (National Institutes of Health, Bethesda, MD, USA) was applied to analyze the intensity of the target bands. β-actin was used as an internal control. The antibodies used were as follows: anti-STK4 (Santa Cruz Technology, Santa Cruz, CA, USA), anti-E-cadherin (Cell Signaling Technology, Danvers, MA, USA), anti-N-cadherin (Cell Signaling Technology), anti-vimentin (Cell Signaling Technology), anti- sex-determining region Y-box 2 (SOX2; Abcam), anti-CD133 (Abcam), anti-Nanog (Abcam), and anti-β-actin (Abcam).

Immunohistochemical (IHC) staining analysis

Tissue samples were fixed in 4% paraformaldehyde overnight and embedded in paraffin according to standard protocols. The paraffin tissue sections were pasted onto glass slides, and then deparaffinized followed by antigen heat retrieval. After inactivating the activity of endogenous peroxidase with 3% H_2O_2 for 10 min, specimens were rinsed three times with PBS and then incubated with Ki67 primary antibody at 1:400 dilution (Cell Signaling Technology) at 4°C overnight. The specimens were then rinsed with PBS and incubated with secondary antibody in a wet box at 37°C for 30 min. After rinsing with PBS again, diaminobenzidine (DAB) was used followed by hematoxylin counterstaining.

Tumor xenograft models

Animal experiments were performed with the approval of the Research Ethics Committee of Nantong University according to the Council on Animal Care Guidelines of Nantong University (approval No. S20200317-019). A total of 24 BALB/c male nude mice (5 weeks old) were housed in a specific pathogen-free grade laboratory at a constant temperature (22°C–25°C) and humidity (55% ± 5%). The mice were randomly divided into four groups (six per group): vector, paclitaxel, GAS5 + saline, and GAS5 + paclitaxel groups. GAS5- or vector-transfected PC3-PR cells were injected subcutaneously into the flanks of the mice (1×10^6 cells per 100 μl per flank). Then 7 days after the inoculation, mice (GAS5 + saline group and GAS5 + paclitaxel group) received either saline (100 μl) or paclitaxel (20 mg kg^{-1}) intraperitoneal injections every 2 days, respectively. Tumor size was measured using vernier calipers for the length (L) and width (W), and the tumor volume (V) was calculated with the formula: $V = L \times W^2 \times 0.5$. All mice were killed and the tumors were isolated and processed for further analysis after 5 weeks. Then tumor tissues were analyzed by IHC for Ki67 protein expression and underwent RNA extraction for qRT-PCR detection.

Statistical analyses

The SPSS 17.0 statistical package was used for statistical analysis in this study (SPSS Inc., Chicago, IL, USA). Quantitative data were indicated as the mean ± standard deviation. Student's *t*-test was used for statistical comparison of two groups, while one-way analysis of variance (ANOVA) was used followed by the Turkey's test when comparing multiple groups. $P < 0.05$ was considered as statistically significantly.

RESULTS

Lower GAS5 expression in PCa is associated with metastasis and paclitaxel resistance

To identify the potential role of GAS5 in PCa, relative GAS5 expression levels were first detected in PCa tissues and cell lines by qRT-PCR. The results showed that the expression of GAS5 was significantly lower in PCa tissues ($n = 36$) than that in normal tissues ($n = 20$; $P < 0.01$; **Figure 1a**). In addition, when the patients were divided into two groups according to their metastasis status (nonmetastasis and

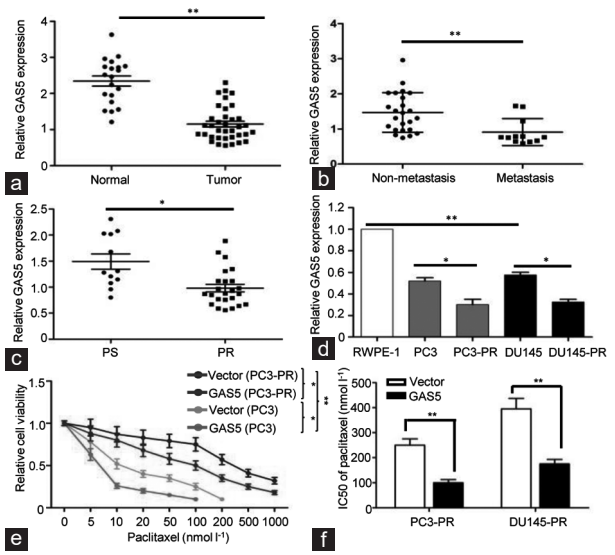

Figure 1: Lower GAS5 expression in PCa is associated with metastasis and PR. (**a**) The relative expression of GAS5 was examined by RT-qPCR in PCa tissues and normal samples. (**b**) GAS5 levels in PCa tissues with or without metastasis were determined by qRT-PCR assay. (**c**) Relative GAS5 expression was detected by qRT-PCR in PR PCa tissues and PS tumor tissues. (**d**) GAS5 was detected in PCa and PR PCa cells by qRT-PCR. (**e**) Survival rates were measured by CCK8 assay in PC3 and PC3-PR cells transfected with pcDNA3.1-GAS5 plasmid or empty vector exposed to the indicated concentrations of paclitaxel for 24 h. (**f**) IC50 values of paclitaxel were analyzed in pcDNA3.1-GAS5 or empty vector-transfected PR PCa cells from the viability versus paclitaxel concentration curves. The data are shown as the mean ± standard deviation. $^*P < 0.05$, $^{**}P < 0.01$. lncRNA: long noncoding RNA; GAS5: lncRNA growth arrest-specific 5; qRT-PCR: quantitative real-time polymerase chain reaction; PR: paclitaxel-resistant; PS: paclitaxel-sensitive; CCK8: cell counting kit-8; IC50: half maximal inhibitory concentration; PCa: prostate cancer.

metastasis), GAS5 expression was significantly lower in patients with metastasis ($n = 12$) than in those with nonmetastasis ($n = 24$; $P < 0.01$; **Figure 1b**). Moreover, to explore the correlation of GAS5 expression and cancer resistance, the patients were classified according to their PR status. The results revealed that relative GAS5 expression levels were markedly lower in PR PCa tissues ($n = 24$) than in paclitaxel-sensitive (PS) tumors ($n = 12$; $P < 0.05$; **Figure 1c**). Similarly, lower expression of GAS5 was also found in PC3 and DU145 cells compared with RWPE-1 normal prostatic epithelial cells, while PC3-PR and DU145-PR cells showed especially lower levels of GAS5 than normal PC3 and DU145 cells, respectively (all $P < 0.05$; **Figure 1d**).

Furthermore, we detected the relative cell viability of PCa and PR PCa cells transfected with pcDNA3.1-GAS5 plasmid (GAS5) or empty vector (vector) by CCK8 assay. The results indicated that GAS5 overexpression conferred the host cells with greater sensitivity to paclitaxel, and the cell viability of PR PCa cells was much higher than that of PCa cells (all $P < 0.05$; **Figure 1e** and **Supplementary Figure 1a**). Likewise, GAS5 remarkably impeded the half maximal inhibitory concentration (IC50) of paclitaxel in both PCa and PR PCa cells (all $P < 0.05$; **Figure 1f** and **Supplementary Figure 1b**). The above results indicated that lower GAS5 in PCa was more prone to metastasis and paclitaxel resistance.

GAS5 suppresses proliferation, colony formation, migration, and invasion, and induces cell cycle arrest of PR PCa cells

To explore the potential effect of GAS5 on chemoresistance in PCa, PC3-PR and DU145-PR cells were transfected with GAS5 or vector and then treated with paclitaxel for 24 h. As a result, GAS5 expression levels were markedly increased in PC3-PR and DU145-PR cells transfected with GAS5 compared with those in the vector group ($P < 0.01$; **Figure 2a**). To evaluate the effects of GAS5 suppression of cell proliferation, CCK-8 assay was performed at 24 h, 48 h, and 72 h after GAS5 transfection. Compared with the nontransfected control (control) and vector group-transfected cells, the marked decrease in cell viability was measured in PC3-PR and DU145-PR cells at 48 h or 72 h after treatment with GAS5. However, no significant difference was found in control and vector-transfected cells at any time point (all $P < 0.05$; **Figure 2b** and **2c**). Next, colony formation assay was performed to further assess the anti-proliferative effects of GAS5 on the proliferation of PR PCa cells. The result showed that the colony numbers of PC3-PR and DU145-PR cells in the GAS5 group were significantly lower than those in the vector group (all $P < 0.01$; **Figure 2d** and **2e**). The above data indicated that GAS5 could suppress the proliferation of PR PCa cells *in vitro*.

To further explore the effect of GAS5 on the cell cycle distribution of PR PCa cells, a flow cytometry assay was performed. In comparison with the vector group, the GAS5-transfected group showed obvious cell cycle arrest in G0/G1 phase at 48 h after transfection. The results indicated that the cell cycle progression from G1 to S phase was blocked following overexpression of GAS5 in PC3-PR and DU145-PR cell lines (all $P < 0.05$; **Figure 2f** and **2g**). Moreover, EdU retention assay was performed to evaluate the effect of GAS5 suppression of DNA replication. Following transfection with GAS5 overexpression plasmid, the percentage of EdU-positive cells was decreased markedly in PC3-PR and DU145-PR cell lines compared with the vector group (all $P < 0.05$; **Figure 2h** and **2i**).

To assess the effect of GAS5 on cell migration, pcDNA3.1-GAS5 plasmid- and empty vector-transfected PR PCa cells were cultured in Transwell chambers. The results revealed that the number of migrated GAS5-transfected PC3-PR and DU145-PR cells was significantly reduced compared with the vector-transfected cells (all $P < 0.01$; **Figure 2j** and **2k**). Similarly, cell invasion detection using a Transwell chamber coated with Matrigel showed that invasive cell numbers were decreased markedly in GAS5-transfected PC3-PR and DU145-PR cells compared with the vector-transfected cells (both $P < 0.01$; **Figure 2l** and **2m**). The data indicated that GAS5 has anti-cancer properties that can inhibit the phenotype of cell migration and invasion in PR PCa cells.

GAS5 inhibits the EMT and stem cell-like characteristics of PR PCa cells

Growing evidence shows that EMT and CSCs have important roles during the chemoresistance and metastasis of PCa.[3,28,29] We investigated whether GAS5 overexpression caused expression changes in EMT and stem cell-like protein markers in PR PCa cells. The results revealed that GAS5 overexpression significantly promoted E-cadherin protein expression while inhibiting N-cadherin and vimentin expression levels (all $P < 0.05$; **Figure 3a** and **3b**), indicating that GAS5 overexpression markedly inhibited EMT.

Evidence has shown that SOX2, CD133, and Nanog are common stem cell-like markers of PCa.[30] The western blotting results demonstrated that the relative protein levels of these markers all decreased significantly (all $P < 0.01$) in the GAS5 overexpression group compared with the vector group, indicating GAS5 repressed the development of stem cell-like phenotypes of PR PCa cells (all $P < 0.01$; **Figure 3c** and **3d**).

GAS5 regulates miR-18a-5p expression and paclitaxel sensitivity by sponging miR-18a-5p in PR PCa cells

Recent studies reported that lncRNAs have suppressing effects on miRNA expression or activity by bearing the complementary sequence to miRNAs.[31–33] To determine whether GAS5 performs a similar function in PR PCa, we predicted the potential interaction between GAS5 and miRNAs using three online resources, ENCORI (http://starbase.sysu.edu.cn/panCancer.php, last accessed on 2021 Jan 15), starBase version 2.0 (http://starbase.sysu.edu.cn/starbase2/index.php, last accessed on 2021 Jan 15), and lncRNA SNP2 (http://bioinfo.life.hust.edu.cn/lncRNASNP/#!/predict, last accessed on 2021 Jan 15). The intersecting result showed the acquisition of eight miRNAs, including miR-18a-5p, miR-18b-5p, miR-4735-3p, and miR-873-5p (**Figure 4a**). We then selected miR-18a-5p as a target according to the top prediction score. Bioinformatics predicted GAS5 RNA contains one conserved binding site of miR-18a-5p. To confirm this possibility, the wild-type sequence of GAS5 (GAS5-WT) or its mutant sequence (GAS5-MUT) as shown in **Figure 4b** was subcloned into a luciferase reporter (pMIR) and co-transfected with miR-18a-5p or miR-CON into PC3-PR and DU145-PR cells. As expected, the relative luciferase activity of pMIR-GAS5-WT declined significantly (all $P < 0.01$) when miR-18a-5p was co-transfected into these cells. However, the GAS5 mutant showed no significant effects on relative luciferase activity between the miR-con and miR-18a-5p mimic groups in PC3-PR and DU145-PR cells (**Figure 4c**).

Recent reports have shown that lncRNAs regulate miRNA activity by forming the RNA-induced silencing complex (RISC).[34–36] To further confirm that GAS5 and miR-18a-5p were included in the RISC, RIP experiments were performed on PC3-PR cellular extracts using an antibody against Ago2, a main component of the RISC.[37] The results revealed that RNA expression levels of GAS5 and miR-18a-5p in Ago2 pellets were all markedly enriched compared with the control IgG immunoprecipitates (all $P < 0.01$; **Figure 4d**). Thus, the data indicate

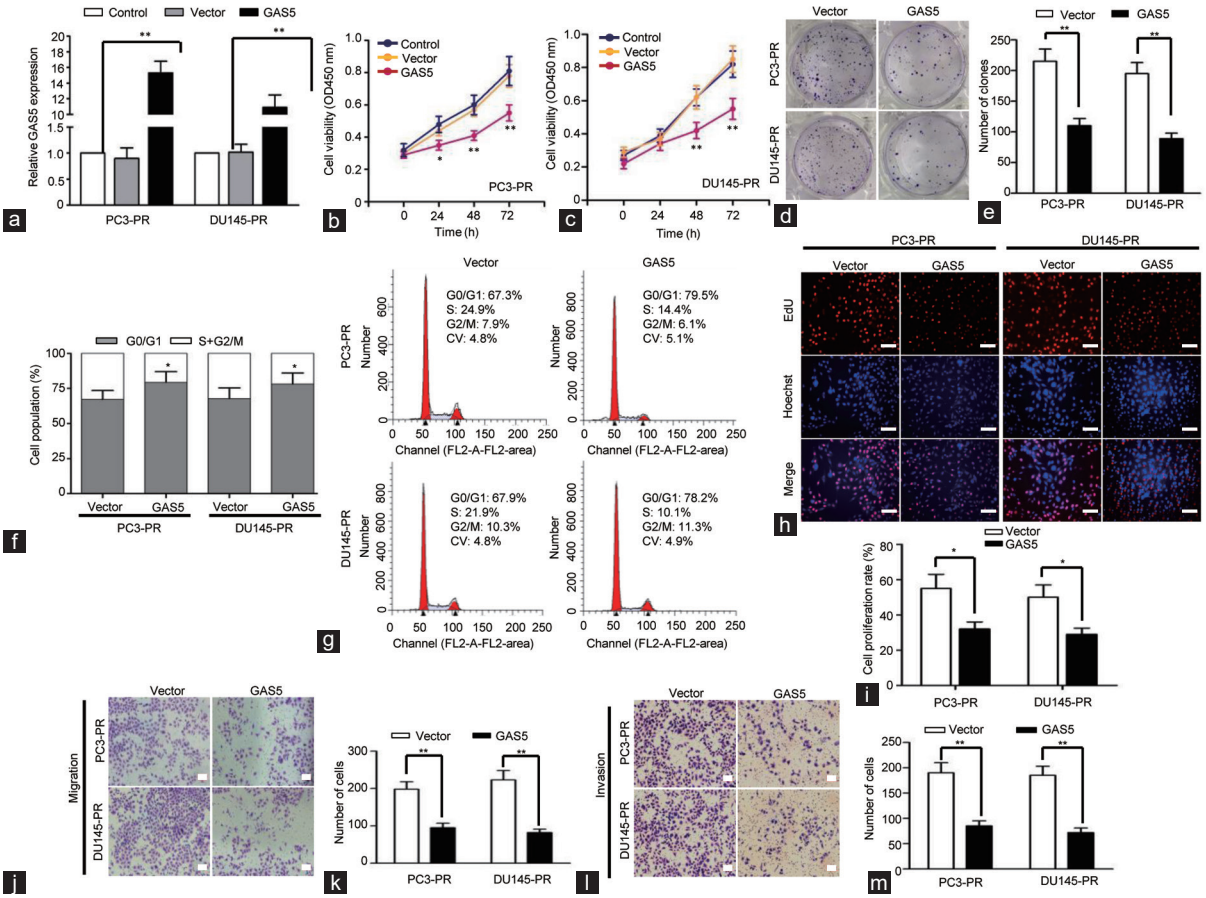

Figure 2: GAS5 suppresses proliferation, colony formation, migration, and invasion and induces cell cycle arrest of PR PCa cells. (**a**) GAS5 expression was detected in PC3-PR and DU145-PR cells transfected with GAS5 or vector by qRT-PCR. Cell viability was measured in (**b**) PC3-PR and **(c)** DU145-PR cells transfected with control, vector, or GAS5 by CCK8 at 0 h, 24 h, 48 h, and 72 h. (**d**) Colony formation assays were performed in PC3-PR and DU145-PR cells transfected with GAS5 or vector. (**e**) Statistical analysis of the colony formation results. (**f**) Statistical analysis of the cell cycle profiles. (**g**) Flow cytometric analysis of cell cycle profiles in PC3-PR and DU145-PR cells transfected with GAS5 or vector. (**h**) Detection of cell proliferation by EdU incorporation assay in PC3-PR and DU145-PR cells transfected with GAS5 or vector. Scale bars = 100 μm. (**i**) Statistical analysis of the EdU results. (**j**) Cell migration was measured in PC3-PR and DU145-PR cells transfected with GAS5 or vector. Scale bars = 100 μm. (**k**) Statistical analysis of the cell migration results. (**l**) Cell invasion was measured in PC3-PR and DU145-PR cells transfected with GAS5 or vector. Scale bars = 100 μm. (**m**) Statistical analysis of the cell invasion results. The data are shown as the mean ± standard deviation. $^{*}P < 0.05$, $^{**}P < 0.01$. lncRNA: long noncoding RNA; GAS5: lncRNA growth arrest-specific 5; qRT-PCR: quantitative real-time polymerase chain reaction; PR: paclitaxel-resistant; CCK8: cell counting kit-8; PCa: prostate cancer; EdU: 5-ethynyl-2'-deoxyuridine.

that GAS5 and miR-18a-5p co-exist in Ago2-containing RISCs and interact with each other, in agreement with the bioinformatic prediction and luciferase assays. Moreover, to further analyze the regulatory relationship between GAS5 and miR-18a-5p in PR PCa, GAS5 RNA was cloned into pcDNA3.1 plasmid and co-transfected into PC3-PR and DU145-PR cells alone with miR-18a-5p. The result showed that GAS5 antagonized miR-18a-5p expression in a dose-dependent manner. However, the vector group showed no significant antagonizing effect on the expression of miR-18a-5p in both PC3-PR and DU145-PR cells (all $P < 0.01$; **Figure 4e**). Taken together, our data indicated that GAS5 may act as an endogenous sponge to restrict miR-18a-5p expression.

To further investigate whether miR-18a-5p is involved in GAS5-addressed chemosensitivity in PCa, PC3-PR and DU145-PR cells were co-transfected with GAS5 or vector and miR-18a-5p or miR-CON. The results demonstrated that miR-18a-5p significantly rescued GAS5-mediated inhibition of the survival rate and paclitaxel IC50 in PC3-PR (all $P < 0.05$; **Figure 4f** and **4g**) and DU145-PR (all $P < 0.05$; **Supplementary Figure 2a** and **2b**) cells after multiple concentrations of paclitaxel for 24 h, indicating miR-18a-5p participated in GAS5-induced chemosensitivity in PCa.

The regulatory relationship between miR-18a-5p and its target STK4

As described above, miR-18a-5p expression was inhibited by GAS5 and participated in GAS5-induced chemosensitivity in PCa. We hypothesized that reduction of miR-18a-5p might decrease repression of its mRNA targets, thus further facilitating the suppressive progression of PCa. Consequently, the target genes of miR-18a-5p were predicted using four online websites, TargetScan (www.targetscan.org, last accessed on 2021 Jan 16), miRDB (http://www.mirdb.org, last accessed on 2021 Jan 16), miRTarBase (http://mirtarbase.mbc.nctu.edu.tw, last accessed on 2021 Jan 16), and PicTar (https://pictar.mdc-berlin.de/, last accessed on 2021 Jan 16), and 17 intersection results were acquired (**Figure 5a**). Among them, we identified *STK4* as a putative target of miR-18a-5p. Dual luciferase reporter assays were then used to verify the predicted accuracy of the bioinformatic findings. The wild type 3'-UTR sequence of *STK4* (STK4-WT) or its mutant sequence (STK4-MUT), as shown in **Figure 5b**, was subcloned into the pMIR luciferase

reporter and then co-transfected with miR-CON, miR-18a-5p, miR-18a-5p + pcDNA-NC, or miR-18a-5p + pcDNA-GAS5 into PC3-PR cells. Compared with the miR-CON group, the relative luciferase activity of STK4-WT was significantly decreased when co-transfected with miR-18a-5p into the cells, indicating that *STK4* was a target of miR-18a-5p. When pMIR-STK4-WT was co-transfected together with miR-18a-5p and pcDNA-GAS5 plasmid into PC3-PR cells, the relative luciferase activity of STK4-WT was rescued partially as compared with the miR-18a-5p and miR-18a-5p + pcDNA-NC groups. However, the relative luciferase activity of STK4-MUT showed no difference in the cells when co-transfected with any vector (all $P < 0.05$; **Figure 5c**).

Several studies have reported that STK4 expression is downregulated in many tumor tissues and that its defect results in carcinogenesis.[38,39] To analyze the protein expression of STK4 in clinical PCa specimens, four fresh PCa tissues (T) and prostate hyperplasia tissues (N) were collected. The western blotting results revealed lower STK4 protein expression in PCa tissues than in prostate hyperplasia tissues (all $P < 0.05$; **Figure 5d**). Data from Gene Expression Profiling Interactive Analysis (GEPIA; http://gepia.cancer-pku.cn/, last accessed on 2021 Jan 16) showed that *STK4* expression was downregulated in tumor tissues ($n = 492$) compared with normal tissues ($n = 152$), as shown in **Figure 5g**.

To further confirm STK4 was involved in miR-18a-5p-mediated proliferation and migration of PR PCa cells, a pcDNA-STK4 overexpression plasmid was constructed and co-transfected with miR-18a-5p or miR-CON into PC3-PR and DU145-PR cells. CCK8 assays indicated that cell proliferation of STK4-transfected PR PCa cells induced by miR-18a-5p was partially reversed (all $P < 0.05$; **Figure 5e** and **5f**). Moreover, the migration results showed similar trends that migrated cell numbers were partially rescued when PR PCa

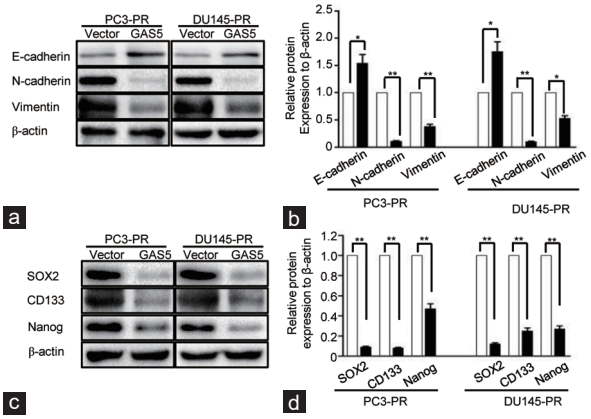

Figure 3: GAS5 inhibits EMT and stem cell-like characteristics of paclitaxel-resistant PCa cells. (**a**) Western blotting of relative EMT-related protein expression and (**b**) statistical analysis of the western blotting results. (**c**) Western blotting of relative stemness marker-related protein expression and (**d**) statistical analysis of the western blotting results. The data are shown as the mean ± standard deviation. $^{*}P < 0.05$, $^{**}P < 0.01$. lncRNA: long noncoding RNA; GAS5: lncRNA growth arrest-specific 5; EMT: epithelial-to-mesenchymal transition; PR: paclitaxel-resistant; SOX2: sex-determining region Y-box 2; PCa: prostate cancer.

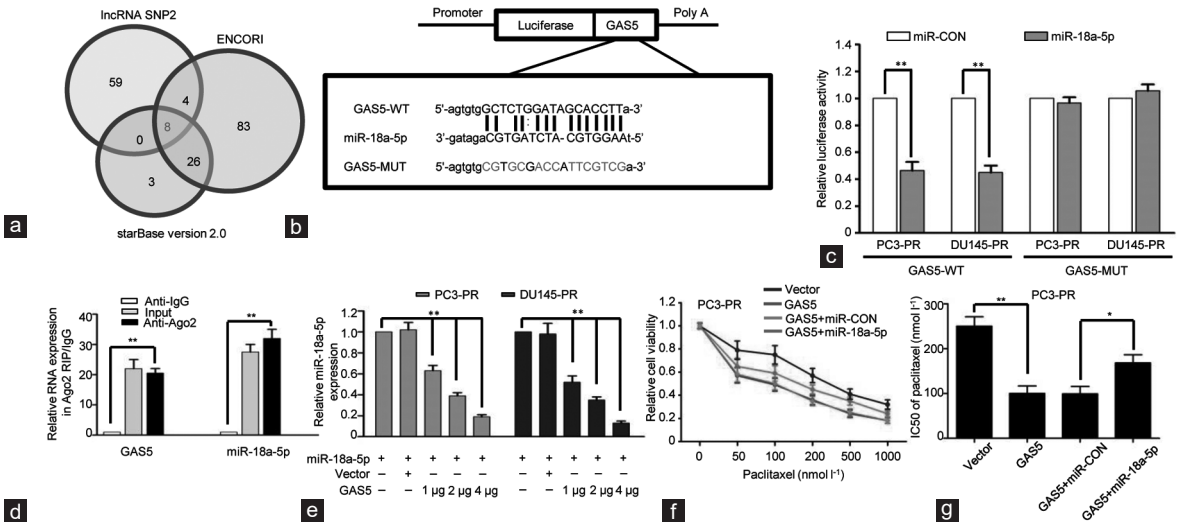

Figure 4: GAS5 regulates miR-18a-5p expression and paclitaxel sensitivity by sponging miR-18a-5p in paclitaxel-resistant PCa cells. (**a**) The predictive potential of miRNAs binding to GAS5 obtained by three online websites lncRNA SNP2, ENCORI, and starBase version 2.0 with default parameters, of which eight miRNAs overlapped. (**b**) Putative miR-18a-5p binding sequence of GAS5 RNA. A human GAS5 RNA containing wild type (WT) or mutant (MUT) miR-18a-5p binding sequence was cloned into pMIR luciferase reporter. (**c**) The wild-type (pMIR-GAS5-WT) and mutant (pMIR-GAS5-MUT) reporter plasmids were co-transfected into PC3-PR and DU145-PR cells with miR-18a-5p or negative control (miR-CON). The normalized luciferase activity was set as relative luciferase activity in the control group. (**d**) RIP experiments were performed in PC3-PR cells with Ago2 antibody. Detection of GAS5 and miR-18a-5p by qRT-PCR. Relative RNA levels are presented as fold enrichment in Ago2 relative to immunoprecipitates of IgG. (**e**) miR-18a-5p (1 μg) was co-transfected into PC3-PR and DU145-PR cells with pcDNA3.1-NC (vector, 1 μg) or pcDNA3.1-GAS5 (GAS5, 1 μg, 2 μg, and 4 μg). The expression of miR-18a-5p was analyzed by qRT-PCR and U6 was used as an internal control. (**f**) The survival rates were detected in PC3-PR cells that were co-transfected with GAS5 or vector and miR-18a-5p or miR-CON by CCK8 assay. (**g**) The IC50 of paclitaxel were detected in PC3-PR cells that were co-transfected with GAS5 or vector and miR-18a-5p or miR-CON by CCK8 assay. The data are s hown as the mean ± standard deviation. $^{*}P < 0.05$, $^{**}P < 0.01$. lncRNA: long noncoding RNA; GAS5: lncRNA growth arrest-specific 5; qRT-PCR: quantitative real-time PCR; PR: paclitaxel-resistant; PS: paclitaxel-sensitive; RIP: RNA immunoprecipitation; Ago2: argonaute 2; U6: U6 small nuclear RNA; CCK8: cell counting kit-8; IC50: half maximal inhibitory concentration; PCa: prostate cancer.

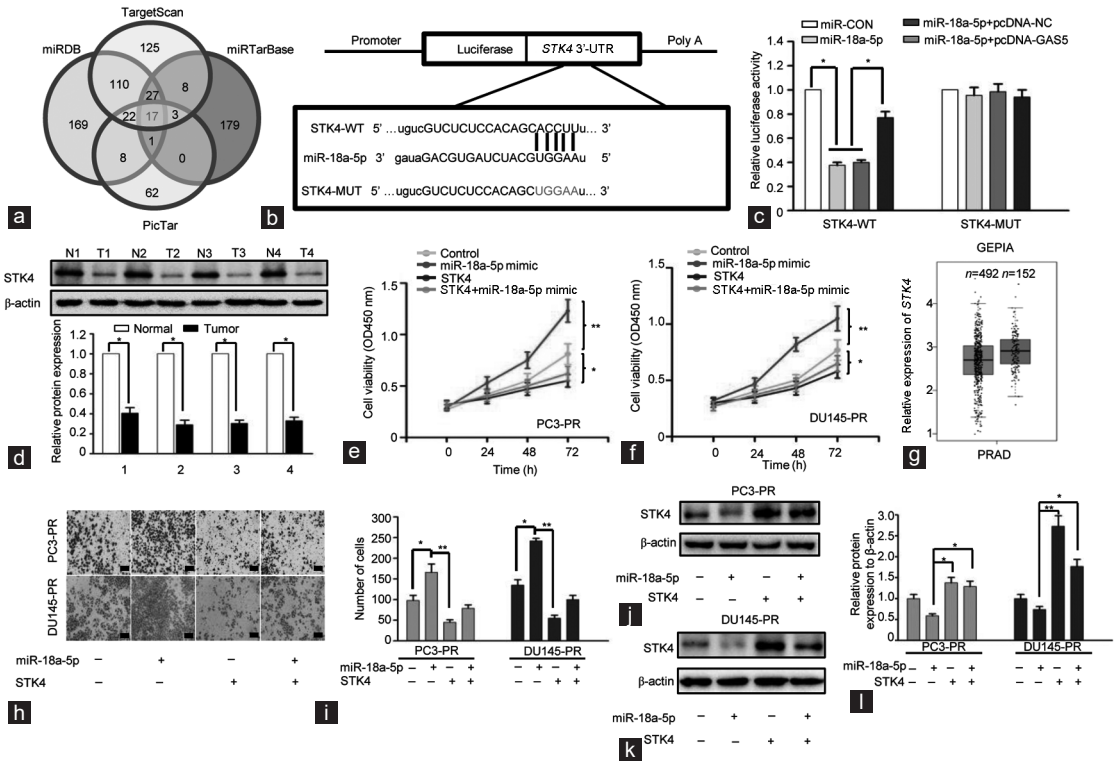

Figure 5: The regulatory relationship between miR-18a-5p and its target STK4. (**a**) The predicted potential target genes of miR-18a-5p from four online websites (TargetScan, miRDB, miRTarBase and PicTar) with default parameters were analyzed. Seventeen genes overlapped. (**b**) Putative miR-18a-5p binding to the 3'-UTR sequence of *STK4* mRNA. A mutation was generated in the *STK4* mRNA 3'-UTR sequence at the complementary site for the seed region of miR-18a-5p. The wild type or mutant miR-18a-5p-binding *STK4* mRNA 3'-UTR sequence was cloned into pMIR luciferase reporter. (**c**) The wild type (STK4/3'-UTR-WT) and mutant (STK4/3'-UTR-Mut) pMIR luciferase reporters were co-transfected into PC3-PR cells with miR-CON, miR-18a-5p, miR-18a-5p, and pcDNA-NC or miR-18a-5p and pcDNA-GAS5. The normalized luciferase activity in the control group was set as relative luciferase activity. (**d**) The relative protein expression of STK4 in clinical PCa specimens, four fresh PCa tissues (T), and benign prostate hyperplasia tissues (N) are shown. Cell viability of (**e**) PC3-PR and (**f**) DU145-PR cell lines transfected with control, miR-18a-5p mimic, STK4 overexpression vector, and STK4 + miR-18a-5p mimic were determined by CCK8 assay at 0 h, 24 h, 48 h, and 72 h. (**g**) *STK4* mRNA expression data from Gene Expression Profiling Interactive Analysis (GEPIA, http://gepia.cancer-pku.cn/) between clinical tumor tissues (n=492) and normal tissues (n=152). (**h**) Transwell assay of PR PCa cells transfected with miR-18a-5p and/or STK4 overexpression vector. Scale bars = 100 μm. (**i**) Statistical analysis of the tranawell assay results. Relative protein expression of STK4 in (**j**) PC3-PR and (**k**) DU145-PR cells transfected with miR-18a-5p and/or STK4 overexpression vector. (**l**) Statistical analysis of the western blotting results. $^{*}P < 0.05$, $^{**}P < 0.01$. 3'-UTR: 3' untranslated regions; STK4: serine/threonine kinase 4; PR: paclitaxel-resistant; CCK8: cell counting kit-8; PCa: prostate cancer; CON: control.

cells were co-transfected with *STK4* and miR-18a-5p (both $P < 0.05$; **Figure 5h** and **5i**). In addition, the western blotting results indicated that STK4 overexpression restored miR-18a-5p-induced downregulation of STK4 in PC3-PR and DU145-PR cells (all $P < 0.05$; **Figure 5j–5l**). These data suggested that miR-18a-5p regulated STK4 expression by directly binding to 3'-UTR of *STK4* mRNA in PR PCa cells.

Verification of the interacting effect of miR-18a-5p and STK4 on paclitaxel resistance in PR PCa cells

To further determine if STK4 was involved in miR-18a-5p-mediated PR PCa cell chemosensitivity, CCK8 assays were performed. The results showed that miR-18a-5p inhibitor enhanced the host cells' chemosensitivity to paclitaxel, while combined miR-18a-5p inhibitor and STK4 treatment exhibited chemosensitivity results to paclitaxel (**Supplementary Figure 3a** and **3b**). Likewise, the IC50 of paclitaxel was markedly decreased when the cells were treated with miR-18a-5p inhibitor and STK4 (both $P < 0.05$; **Supplementary Figure 3c** and **3d**). The data suggested synergy between miR-18a-5p inhibitor and STK4 caused enhanced paclitaxel sensitivity, as indicated by the reduced IC50.

Moreover, western blotting results showed that STK4 overexpression antagonized miR-18a-5p-induced N-cadherin and vimentin expression but reversed E-cadherin epithelial marker expression (both $P < 0.05$; **Supplementary Figure 3e** and **3f**), which indicated that STK4 expression inhibited EMT. Western blotting also showed that STK4 overexpression antagonized miR-18a-5p-induced SOX2 and CD133 expression (both $P < 0.05$; **Supplementary Figure 3g** and **3h**). Collectively, the data indicated that STK4 enhanced cancer cell chemosensitivity by inhibiting EMT and the stem cell-like phenotype via antagonizing miR-18a-5p.

GAS5 overexpression inhibits the tumor growth of xenografts and elevates PCa sensitivity to paclitaxel

To further explore the anti-tumor effects of GAS5 on xenograft growth and sensitivity to paclitaxel, a BALB/c nude mice xenograft experiment was performed by subcutaneous injection of PC3-PR cells carrying GAS5 or vector and then treated with paclitaxel. The results showed that paclitaxel treatment alone resulted in no anti-tumor effect because of the chemoresistance of PC3-PR cells to paclitaxel. However, GAS5 overexpression effectively impeded tumor growth compared with the vector group, and GAS5 combined with paclitaxel treatment resulted in the most effective tumor inhibition in the four groups (all $P < 0.05$; **Figure 6a–6c**).

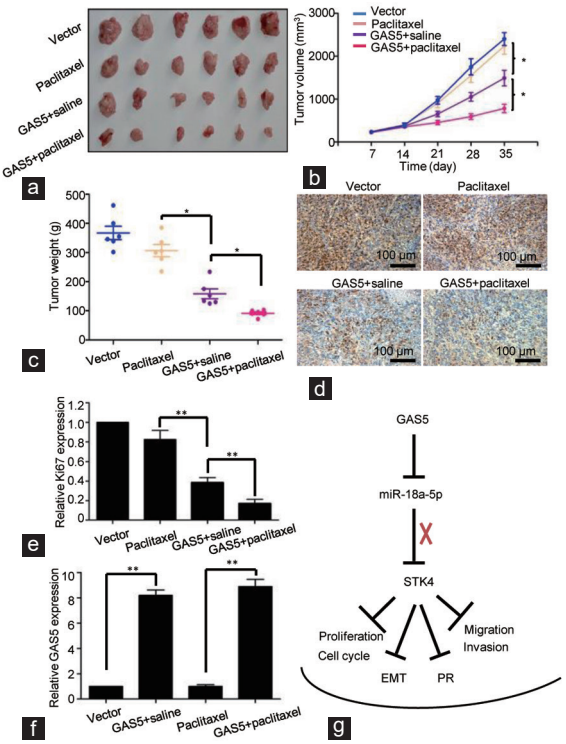

Figure 6: GAS5 overexpression inhibits tumor growth of xenografts and paclitaxel resistance. (**a**) Images of tumor xenografts 35 days after inoculation of the four groups. (**b**) Tumor growth curves of PC3-PR cells transfected with GAS5 overexpression plasmid or empty vector and treated with paclitaxel (20 mg kg^{-1}) or saline. (**c**) Tumor weights were compared between the four groups. (**d**) Ki67 expression of tumor growth in the four groups detected by IHC. Scale bars = 100 μm. (**e**) Statistical analysis of the IHC results. (**f**) Relative GAS5 expression in tumor tissues in the four groups by qRT-PCR detection. (**g**) Diagram depicting an intuitive regulatory network of GAS5/miR-18a-5p/STK4 in PCa that inhibits EMT and enhances tumor stem cell-like-mediated sensitivity of paclitaxel. $^{*}P < 0.05$, $^{**}P < 0.01$. lncRNA: long noncoding RNA; GAS5: lncRNA growth arrest-specific 5; EMT: epithelial-to-mesenchymal transition; PR: paclitaxel-resistant; IHC: immunohistochemistry; PCa: prostate cancer.

Moreover, immunostaining analysis of proliferation-associated antigen Ki67 and RT-qPCR analysis of GAS5 expression were performed in resected tumor tissues from the four groups. The Ki67 staining results indicated that GAS5 treatment decreased the Ki67-positive rate markedly, while the GAS5 + paclitaxel treatment group obtained the lowest Ki67-positive rate compared with the other groups (all $P < 0.01$; **Figure 6d** and **6e**). Finally, the RT-qPCR results verified that GAS5 expression levels in tumors that originated from GAS5-transfected PC3-PR cells was significantly higher than that in tumors from non-GAS5-transfected cells ($P < 0.01$; **Figure 6f**). The experimental data revealed that GAS5 inhibited tumor growth and enhanced the sensitivity of PR PCa cells to paclitaxel *in vivo*.

DISCUSSION

Chemotherapy resistance commonly occurs during various cancer treatments in the clinic.[40–42] Paclitaxel is a microtubule-targeting chemotherapeutic drug that can be used for the clinical treatment of PCa. Although it is now not a standard drug for PCa patients compared with docetaxel or cabazitaxel, it still has clinical significance for research purposes. Paclitaxel chemoresistance often occurs during treatment and seriously affects the prognosis of patients.[43,44] Increasing evidence have shown that lncRNAs play vital roles in the progression of cancer regulation and chemotherapy resistance.[20,35,45] In this study, we found that the lncRNA GAS5 acts as a tumor suppressor and significantly suppressed PCa progression and paclitaxel resistance by inhibiting EMT and CSC properties.

GAS5 has been reported to be downregulated in multiple cancers.[46,47] However, its molecular function in PR PCa has not been investigated. Our experimental results demonstrated that GAS5 expression levels were lower in PCa tissues and especially in patients with metastasis and paclitaxel resistance, indicating that lower GAS5 expression could be related to paclitaxel chemoresistance. Then, PR PCa cell lines (PC3-PR and DU145-PR cells) were constructed and used for the subsequent experiments. Consistently, relative GAS5 expression levels were markedly lower in the PR PCa cell lines and GAS5 overexpression remarkably impeded the IC50 of paclitaxel in both PCa and PR PCa cells. The data further indicated that GAS5 may have an important role in the paclitaxel chemoresistance of PCa. In addition, we identified the comprehensive function of GAS5 in PR PCa cells by applying gain-of-function approaches. GAS5 overexpression markedly suppressed proliferation, colony formation, migration, and invasion and induced cell cycle arrest of the PR PCa cells. Similar to the report by Luo *et al*.[48] our data showed that GAS5 expression was significantly downregulated in prostate cancer cells compared with prostate epithelial cells, and ectopic GAS5 expression inhibited cell proliferation and induced cell-cycle arrest in G–S phase, whereas GAS5 knockdown promoted the G–S phase transition. Interestingly, Zhang *et al*.[49] demonstrated that GAS5-007 knockdown inhibited proliferation and cell-cycle progression and promoted cell apoptosis of PCa. We believe that these experimental results may be largely due to the choice of GAS5 transcript (ENST00000456293.5, GAS5-007), while our research transcript is based on the GAS5 sequence NR_002578.3, ENST00000450589.5, in NCBI. Moreover, we found that GAS5 inhibited the protein expression of EMT and stem cell-like markers in PR PCa cells. This is the first study to elucidate the functional significance of GAS5 expression in PR PCa, and the findings demonstrated that GAS5 functions as a tumor suppressor and suppresses PR PCa malignant progression. GAS5 inhibits EMT and enhances the tumor stem cell-like-mediated sensitivity of paclitaxel in PCa. Therefore, GAS5 holds great promise as a novel adjuvant therapeutic target for PR PCa.

Accumulating evidence indicates that lncRNAs regulate the expression of their genes by functioning as a competing endogenous RNA (ceRNA) for miRNA or by interacting with RNA-binding proteins.[50,51] In this study, from this perspective, we explored the molecular mechanism that GAS5 acts as a tumor suppressor and inhibits EMT and enhances the tumor stem cell-like-mediated sensitivity of paclitaxel. Then, through bioinformatics and experimental verification, we determined that miR-18a-5p was one of the GAS5 sponging targets. Our research results confirmed that miR-18a-5p participated in GAS5-induced chemosensitivity in PCa. Studies have shown that miR-18a-5p promotes oncogenic activity in various cancers.[52–54] Another study showed that lncRNA Fer-1-like family member 4 (*FER1L4*) suppresses EMT via inhibiting miR-18a-5p in osteosarcoma,[55] and this result is consistent, in part, with our findings in PR PCa.

Moreover, the experiments further verified the changes in miR-18a-5p expression levels in PR PCa cell lines, directly affecting the expression of one of its downstream targets, STK4 (mammalian sterile 20-like kinase 1).[56] It has been identified as a tumor suppressor in multiple cancers,[39,57] as in PCa. In addition, the interaction effect between miR-18a-5p and STK4 suggested synergy between miR-18a-5p inhibitor and STK4 caused enhanced paclitaxel sensitivity by reducing the IC50.

Thus, the data further indicate that the GAS5/miR-18a-5p/STK4 axis may play a vital role in regulating EMT and the tumor stem cell-like-mediated sensitivity of paclitaxel in PR PCa.

CONCLUSIONS

In summary, our present study highlights that GAS5 acts as a tumor suppressor by suppressing the malignant progression of PCa; notably, mechanistic analysis indicates a novel regulatory network of GAS5/miR-18a-5p/STK4 in PCa that inhibits EMT and enhances the tumor stem cell-like-mediated sensitivity to paclitaxel (**Figure 6g**). However, we recognize that the GAS5/miR-18a-5p/STK4 axis is not the only pathway involved because GAS5 may potentially regulate large numbers of miRNAs, while one miRNA may target lots of genes. They are all involved in cross-talk pathways in a complex and elaborate regulatory network in PCa. Therefore, further efforts should be made to better enhance the sensitivity of chemotherapy drugs and inhibit EMT in PR PCa. In brief, our findings provide novel direction for the development of a potential adjunct to cancer chemotherapy that aims to improve the sensitivity of chemotherapy drugs in PCa.

AUTHOR CONTRIBUTIONS

TTL and XT mainly participated in the experimental design and *in vitro* experiments and drafted the manuscript. HLL performed qRT-PCR, western blotting, and dual-luciferase assays. LG collected the patient samples and participated in the data analysis. HH performed *in vivo* experiments and immunohistochemical analyses. FL designed the study, performed the EdU and flow cytometry analyses, and revised the manuscript. All authors read and approved the final manuscript.

COMPETING INTERESTS

All authors declared no competing interests.

ACKNOWLEDGMENTS

This study was supported by the Nantong Science and Technology Project (No. JC2020027, No. MS12018066, and No. MSZ19216).

Supplementary Information is linked to the online version of the paper on the *Asian Journal of Andrology* website.

REFERENCES

1 Siegel RL, Miller KD, Jemal A. Cancer statistics, 2018. *CA Cancer J Clin* 2018; 68: 7–30.
2 Attard G, Parker C, Eeles RA, Schroder F, Tomlins SA, *et al*. Prostate cancer. *Lancet* 2016; 387: 70–82.
3 Paranjape AN, Soundararajan R, Werden SJ, Joseph R, Taube JH, *et al*. Inhibition of FOXC2 restores epithelial phenotype and drug sensitivity in prostate cancer cells with stem-cell properties. *Oncogene* 2016; 35: 5963–76.
4 Litwin MS, Tan HJ. The diagnosis and treatment of prostate cancer: a review. *JAMA* 2017; 317: 2532–42.
5 Li H, Qian Y, Wang X, Pi R, Zhao X, *et al*. Targeted activation of Stat3 in combination with paclitaxel results in increased apoptosis in epithelial ovarian cancer cells and a reduced tumour burden. *Cell Prolif* 2020; 53: e12719.
6 Wanderley CW, Colon DF, Luiz JP, Oliveira FF, Viacava PR, *et al*. Paclitaxel reduces tumor growth by reprogramming tumor-associated macrophages to an M1 profile in a TLR4-dependent manner. *Cancer Res* 2018; 78: 5891–900.
7 Xue YN, Yu BB, Liu YN, Guo R, Li JL, *et al*. Zinc promotes prostate cancer cell chemosensitivity to paclitaxel by inhibiting epithelial-mesenchymal transition and inducing apoptosis. *Prostate* 2019; 79: 647–56.
8 Pu J, Shen J, Zhong Z, Yanling M, Gao J. KANK1 regulates paclitaxel resistance in lung adenocarcinoma A549 cells. *Artif Cells Nanomed Biotechnol* 2020; 48: 639–47.
9 Feng Q, Li X, Sun W, Sun M, Li Z, *et al*. Targeting G6PD reverses paclitaxel resistance in ovarian cancer by suppressing GSTP1. *Biochem Pharmacol* 2020; 178: 114092.
10 Samli H, Samli M, Vatansever B, Ardicli S, Aztopal N, *et al*. Paclitaxel resistance and the role of miRNAs in prostate cancer cell lines. *World J Urol* 2019; 37: 1117–26.
11 Gasca J, Flores ML, Jimenez-Guerrero R, Saez ME, Barragan I, *et al*. EDIL3 promotes epithelial-mesenchymal transition and paclitaxel resistance through its interaction with integrin alphaVbeta3 in cancer cells. *Cell Death Discov* 2020; 6: 86.
12 Liu L, Zhu H, Liao Y, Wu W, Liu L, *et al*. Inhibition of Wnt/beta-catenin pathway reverses multi-drug resistance and EMT in Oct4$^+$/Nanog$^+$ NSCLC cells. *Biomed Pharmacother* 2020; 127: 110225.
13 Lee YS, Kim SM, Kim BW, Chang HJ, Kim SY, *et al*. Anti-cancer effects of HNHA and lenvatinib by the suppression of EMT-mediated drug resistance in cancer stem cells. *Neoplasia* 2018; 20: 197–206.
14 Nagano T, Fraser P. No-nonsense functions for long noncoding RNAs. *Cell* 2011; 145: 178–81.
15 Ponting CP, Oliver PL, Reik W. Evolution and functions of long noncoding RNAs. *Cell* 2009; 136: 629–41.
16 Fatica A, Bozzoni I. Long non-coding RNAs: new players in cell differentiation and development. *Nat Rev Genet* 2014; 15: 7–21.
17 Jiang C, Li X, Zhao H, Liu H. Long non-coding RNAs: potential new biomarkers for predicting tumor invasion and metastasis. *Mol Cancer* 2016; 15: 62.
18 Dykes IM, Emanueli C. Transcriptional and post-transcriptional gene regulation by long non-coding RNA. *Genomics Proteomics Bioinformatics* 2017; 15: 177–86.
19 Mourtada-Maarabouni M, Williams GT. Growth arrest on inhibition of nonsense-mediated decay is mediated by noncoding RNA GAS5. *Biomed Res Int* 2013; 2013: 358015.
20 Liu B, Wu S, Ma J, Yan S, Xiao Z, *et al*. lncRNA GAS5 reverses EMT and tumor stem cell-mediated gemcitabine resistance and metastasis by targeting miR-221/SOCS3 in pancreatic cancer. *Mol Ther Nucleic Acids* 2018; 13: 472–82.
21 Chen K, Rajewsky N. The evolution of gene regulation by transcription factors and microRNAs. *Nat Rev Genet* 2007; 8: 93–103.
22 Stojanovic J, Tognetto A, Tiziano DF, Leoncini E, Posteraro B, *et al*. MicroRNAs expression profiles as diagnostic biomarkers of gastric cancer: a systematic literature review. *Biomarkers* 2019; 24: 110–9.
23 Harrandah AM, Mora RA, Chan EK. Emerging microRNAs in cancer diagnosis, progression, and immune surveillance. *Cancer Lett* 2018; 438: 126–32.
24 Zhang H, Cai K, Wang J, Wang X, Cheng K, *et al*. MiR-7, inhibited indirectly by lincRNA HOTAIR, directly inhibits SETDB1 and reverses the EMT of breast cancer stem cells by downregulating the STAT3 pathway. *Stem Cells* 2014; 32: 2858–68.
25 Dermani FK, Amini R, Saidijam M, Pourjafar M, Saki S, *et al*. Zerumbone inhibits epithelial-mesenchymal transition and cancer stem cells properties by inhibiting the beta-catenin pathway through miR-200c. *J Cell Physiol* 2018; 233: 9538–47.
26 Fu H, Fu L, Xie C, Zuo WS, Liu YS, *et al*. miR-375 inhibits cancer stem cell phenotype and tamoxifen resistance by degrading HOXB3 in human ER-positive breast cancer. *Oncol Rep* 2017; 37: 1093–9.
27 Takeda M, Mizokami A, Mamiya K, Li YQ, Zhang J, *et al*. The establishment of two paclitaxel-resistant prostate cancer cell lines and the mechanisms of paclitaxel resistance with two cell lines. *Prostate* 2007; 67: 955–67.
28 Li P, Yang R, Gao WQ. Contributions of epithelial-mesenchymal transition and cancer stem cells to the development of castration resistance of prostate cancer. *Mol Cancer* 2014; 13: 55.
29 Marin-Aguilera M, Codony-Servat J, Reig O, Lozano JJ, Fernandez PL, *et al*. Epithelial-to-mesenchymal transition mediates docetaxel resistance and high risk of relapse in prostate cancer. *Mol Cancer Ther* 2014; 13: 1270–84.
30 Harris KS, Kerr BA. Prostate cancer stem cell markers drive progression, therapeutic resistance, and bone metastasis. *Stem Cells Int* 2017; 2017: 8629234.
31 Hou P, Zhao Y, Li Z, Yao R, Ma M, *et al*. LincRNA-ROR induces epithelial-to-mesenchymal transition and contributes to breast cancer tumorigenesis and metastasis. *Cell Death Dis* 2014; 5: e1287.
32 Liz J, Portela A, Soler M, Gomez A, Ling H, *et al*. Regulation of pri-miRNA processing by a long noncoding RNA transcribed from an ultraconserved region. *Mol Cell* 2014; 55: 138–47.
33 Thomson DW, Dinger ME. Endogenous microRNA sponges: evidence and controversy. *Nat Rev Genet* 2016; 17: 272–83.
34 Cesana M, Cacchiarelli D, Legnini I, Santini T, Sthandier O, *et al*. A long noncoding RNA controls muscle differentiation by functioning as a competing endogenous RNA. *Cell* 2011; 147: 358–69.
35 Zhao CC, Jiao Y, Zhang YY, Ning J, Zhang YR, *et al*. Lnc SMAD5-AS1 as ceRNA inhibit proliferation of diffuse large B cell lymphoma via Wnt/beta-catenin pathway by sponging miR-135b-5p to elevate expression of APC. *Cell Death Dis* 2019; 10: 252.
36 Kallen AN, Zhou XB, Xu J, Qiao C, Ma J, *et al*. The imprinted H19 lncRNA antagonizes let-7 microRNAs. *Mol Cell* 2013; 52: 101–12.
37 Lingel A, Izaurralde E. RNAi: finding the elusive endonuclease. *RNA* 2004; 10: 1675–9.
38 Li W, Xiao J, Zhou X, Xu M, Hu C, *et al*. STK4 regulates TLR pathways and protects against chronic inflammation-related hepatocellular carcinoma. *J Clin Invest* 2015; 125: 4239–54.
39 Lin CH, Hsu TI, Chiou PY, Hsiao M, Wang WC, *et al*. Downregulation of STK4 promotes colon cancer invasion/migration through blocking beta-catenin degradation. *Mol Oncol* 2020; 14: 2574–88.
40 Yue J, Vendramin R, Liu F, Lopez O, Valencia MG, *et al*. Targeted chemotherapy overcomes drug resistance in melanoma. *Genes Dev* 2020; 34: 637–49.
41 Goka ET, Chaturvedi P, Lopez DT, Garza A, Lippman ME. RAC1b overexpression confers resistance to chemotherapy treatment in colorectal cancer. *Mol Cancer*

Ther 2019; 18: 957–68.
42 Riesco-Martinez M, Parra K, Saluja R, Francia G, Emmenegger U. Resistance to metronomic chemotherapy and ways to overcome it. *Cancer Lett* 2017; 400: 311–8.
43 Obasaju C, Hudes GR. Paclitaxel and docetaxel in prostate cancer. *Hematol Oncol Clin North Am* 2001; 15: 525–45.
44 Flores ML, Castilla C, Gasca J, Medina R, Perez-Valderrama B, *et al*. Loss of PKCdelta induces prostate cancer resistance to paclitaxel through activation of Wnt/beta-cateninpathway and Mcl-1 accumulation. *Mol Cancer Ther* 2016; 15: 1713–25.
45 Shang AQ, Wang WW, Yang YB, Gu CZ, Ji P, *et al*. Knockdown of long noncoding RNA PVT1 suppresses cell proliferation and invasion of colorectal cancer via upregulation of microRNA-214-3p. *Am J Physiol Gastrointest Liver Physiol* 2019; 317: G222–32.
46 Fang P, Xiang L, Chen W, Li S, Huang S, *et al*. LncRNA GAS5 enhanced the killing effect of NK cell on liver cancer through regulating miR-544/RUNX3. *Innate Immun* 2019; 25: 99–109.
47 Liu Y, Yin L, Chen C, Zhang X, Wang S. Long non-coding RNA GAS5 inhibits migration and invasion in gastric cancer via interacting with p53 protein. *Dig Liver Dis* 2020; 52: 331–8.
48 Luo G, Liu D, Huang C, Wang M, Xiao X, *et al*. LncRNA GAS5 inhibits cellular proliferation by targeting $P27^{Kip1}$. *Mol Cancer Res* 2017; 15: 789–99.
49 Zhang Y, Su X, Kong Z, Fu F, Zhang P, *et al*. An androgen reduced transcript of LncRNA GAS5 promoted prostate cancer proliferation. *PLoS One* 2017; 12: e0182305.
50 Yang F, Shen Y, Zhang W, Jin J, Huang D, *et al*. An androgen receptor negatively induced long non-coding RNA ARNILA binding to miR-204 promotes the invasion and metastasis of triple-negative breast cancer. *Cell Death Differ* 2018; 25: 2209–20.
51 Lv M, Zhong Z, Huang M, Tian Q, Jiang R, *et al*. lncRNA H19 regulates epithelial-mesenchymal transition and metastasis of bladder cancer by miR-29b-3p as competing endogenous RNA. *Biochim Biophys Acta Mol Cell Res* 2017; 1864: 1887–99.
52 Yin SL, Xiao F, Liu YF, Chen H, Guo GC. Long non-coding RNA FENDRR restrains the aggressiveness of CRC via regulating miR-18a-5p/ING4 axis. *J Cell Biochem* 2019. Doi: 10.1002/jcb.29555. [Online ahead of print].
53 Liu Q, Yu W, Zhu S, Cheng K, Xu H, *et al*. Long noncoding RNA GAS5 regulates the proliferation, migration, and invasion of glioma cells by negatively regulating miR-18a-5p. *J Cell Physiol* 2018; 234: 757–68.
54 Zhou L, Li Z, Pan X, Lai Y, Quan J, *et al*. Identification of miR-18a-5p as an oncogene and prognostic biomarker in RCC. *Am J Transl Res* 2018; 10: 1874–86.
55 Ye F, Tian L, Zhou Q, Feng D. LncRNA FER1L4 induces apoptosis and suppresses EMT and the activation of PI3K/AKT pathway in osteosarcoma cells via inhibiting miR-18a-5p to promote SOCS5. *Gene* 2019; 721: 144093.
56 Creasy CL, Ambrose DM, Chernoff J. The Ste20-like protein kinase, Mst1, dimerizes and contains an inhibitory domain. *J Biol Chem* 1996; 271: 21049–53.
57 Morgan EL, Patterson MR, Ryder EL, Lee SY, Wasson CW, *et al*. MicroRNA-18a targeting of the STK4/MST1 tumour suppressor is necessary for transformation in HPV positive cervical cancer. *PLoS Pathog* 2020; 16: e1008624.

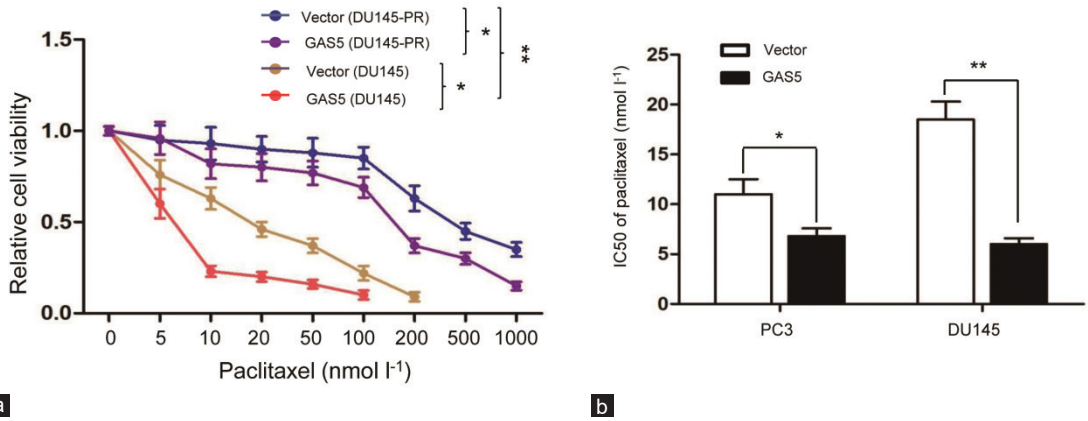

Supplementary Figure 1: GAS5 expression in PCa is associated with paclitaxel resistance. (**a**) Survival rates were measured by CCK8 assay in DU145-PR and DU145 cells transfected with pcDNA3.1-GAS5 plasmid or empty vector exposed to the indicated concentrations of paclitaxel for 24 h. (**b**) IC50 values of paclitaxel were analyzed in pcDNA3.1-GAS5 or empty vector-transfected PCa cells from the viability versus paclitaxel concentration curves. The data are shown as the mean ± standard deviation. $^{*}P < 0.05$, $^{**}P < 0.01$. lncRNA: long noncoding RNA; GAS5: lncRNA growth arrest-specific 5; PR: paclitaxel-resistant; CCK8: cell counting kit-8; IC50: half maximal inhibitory concentration; PCa: prostate cancer.

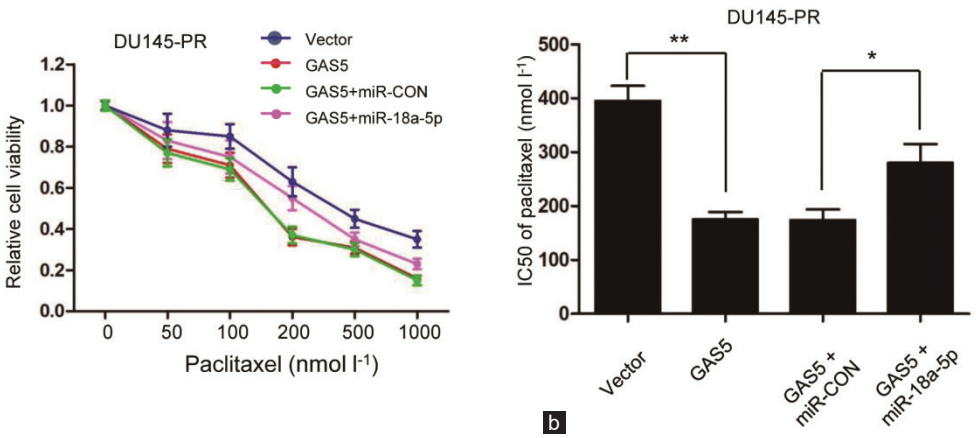

Supplementary Figure 2: Results of the survival rates and IC50 of paclitaxel in DU145-PR cells after the transfection. (**a**) The survival rates were detected in DU145-PR cells that were co-transfected with GAS5 or vector and miR-18a-5p or miR-CON by CCK8 assay. (**b**) The IC50 of paclitaxel were detected in DU145-PR cells that were co-transfected with GAS5 or vector and miR-18a-5p or miR-CON by CCK8 assay. The data are shown as the mean ± standard deviation. $^{*}P < 0.05$, $^{**}P < 0.01$. lncRNA: long noncoding RNA; GAS5: lncRNA growth arrest-specific 5; PR: paclitaxel-resistant; CCK8: cell counting kit-8; IC50: half maximal inhibitory concentration; PCa: prostate cancer.

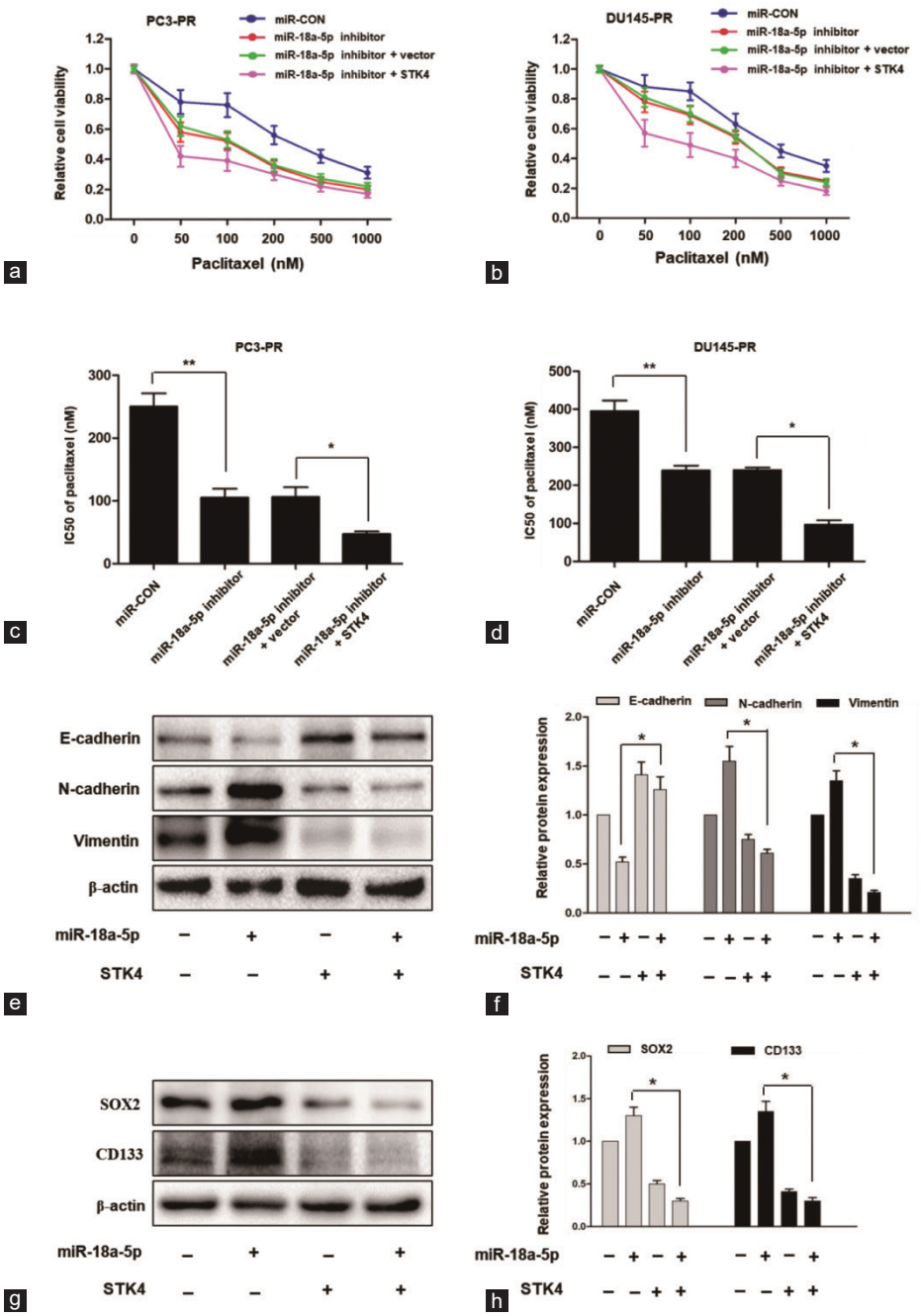

Supplementary Figure 3: Verification of the interacting effects of miR-18a-5p and *STK4* on paclitaxel resistance in paclitaxel-resistant PCa cells. Survival rates were determined in (**a**) PC3-PR and (**b**) DU145-PR cells co-transfected with miR-18a-5p inhibitor and *STK4* or vector by CCK8 assay. IC50 values of paclitaxel were measured in (**c**) PC3-PR and (**d**) DU145-PR cells co-transfected with miR-18a-5p inhibitor and *STK4* or vector by CCK8 assay. (**e**) Western blotting of E-cadherin, N-cadherin, and vimentin protein expression. (**f**) Statistical analysis of the western blotting results. (**g**) Western blotting of SOX2 and CD133 protein expression. (**h**) Statistical analysis of the western blotting results. The data are shown as the mean ± standard deviation. $^{*}P < 0.05$, $^{**}P < 0.01$. lncRNA: long noncoding RNA; GAS5: lncRNA growth arrest-specific 5; PR: paclitaxel-resistant; CCK8: cell counting kit-8; IC50: half maximal inhibitory concentration; SOX2: sex-determining region Y-box 2; STK4: serine/threonine kinase 4; PCa: prostate cancer.